Received: 20 June 2022 | Revised: 14 September 2022 | Accepted: 15 September 2022

DOI: 10.1002/pro.4454

FOR THE RECORD

A method for selective ^{19}F-labeling absent of probe sequestration (SLAPS)

Austin D. Dixon[1] | **Scott A. Robson**[1] | **Jonathan C. Trinidad**[2] | **Joshua J. Ziarek**[1]

[1]Department of Molecular and Cellular Biochemistry, Indiana University, Bloomington, Indiana, USA

[2]Laboratory for Biological Mass Spectrometry, Department of Chemistry, Indiana University, Bloomington, Indiana, USA

Correspondence
Joshua J. Ziarek, Department of Molecular and Cellular Biochemistry, Indiana University, Simon Hall, Lab 301, 212 S. Hawthorne Drive, Bloomington, Indiana 47405, USA.
Email: jjziarek@indiana.edu

Funding information
Indiana University Fund; National Institutes of Health, Grant/Award Numbers: R35GM143054, R00GM115814; Indiana Precision Health Initiative

Review Editor: Hideo Akutsu

Abstract

Fluorine (^{19}F) offers several distinct advantages for biomolecular nuclear magnetic resonance spectroscopy such as no background signal, 100% natural abundance, high sensitivity, and a large chemical shift range. Exogenous cysteine-reactive ^{19}F-probes have proven especially indispensable for characterizing large, challenging systems that are less amenable to other isotopic labeling strategies such as G protein-coupled receptors. As fluorine linewidths are inherently broad, limiting reactions with offsite cysteines is critical for spectral simplification and accurate deconvolution of component peaks—especially when analyzing systems with intermediate to slow timescale conformational exchange. Here, we uncovered noncovalent probe sequestration by detergent proteomicelles as a second source of offsite labeling when using the popular ^{19}F-probe BTFMA (2-bromo-N-(4-[trifluoromethyl]phenyl)acetamide). The chemical shift and relaxation rates of these unreacted ^{19}F-BTFMA molecules are insufficient to distinguish them from protein-conjugates, but they can be easily identified using mass spectrometry. We present a simple four-step protocol for Selective Labeling Absent of Probe Sequestration (SLAPS): physically disrupt cell membranes in the absence of detergent, incubate membranes with cysteine-reactive ^{19}F-BTFMA, remove excess unreacted ^{19}F-BTFMA molecules via ultracentrifugation, and finally solubilize in the detergent of choice. Our approach builds upon the in-membrane chemical modification method with the addition of one crucial step: removal of unreacted ^{19}F-probes by ultracentrifugation *prior to* detergent solubilization. SLAPS is broadly applicable to other lipophilic cysteine-reactive probes and membrane protein classes solubilized in detergent micelles or lipid mimetics.

Statement: Labeling detergent-solubilized proteins with cysteine-reactive ^{19}F NMR probes can result in offsite incorporation and ambiguous spectral results. We demonstrate a second mechanism of offsite labeling when using the ^{19}F-probe BTFMA: noncovalent probe sequestration by detergent proteomicelles. We report a simple protocol for selective labeling that avoids ^{19}F-BTFMA sequestration. This method is broadly applicable to other lipophilic cysteine-reactive probes and membrane protein classes solubilized in detergent micelles or lipid mimetics.

KEYWORDS

2-bromo-N-(4-[trifluoromethyl]phenyl)acetamide, detergent, G protein-coupled receptor, in-membrane chemical modification, isotope labeling, lipid mimetic, lipophilic, mass spectrometry, membrane protein, micelle, nuclear magnetic resonance

1 | INTRODUCTION

G protein-coupled receptors (GPCRs) are the largest integral membrane protein class in eukaryotes with over 800 unique members that regulate numerous biological processes including mood, body temperature, taste, and sight, among others.[1,2] They share a conserved architecture of seven transmembrane (TM) alpha-helices that bundle together to form an extracellular orthosteric binding pocket and an intracellular cytosolic cleft.[3] Ligand binding at the orthosteric pocket induces a conformational change at the intracellular cleft to enable G protein association, guanine nucleotide exchange, and ultimately an intracellular signaling cascade. Termination of GPCR signaling is mediated through ternary complex formation with arrestin, which activates clathrin-mediated endocytosis for receptor recycling/degradation.[2] Due to their broad physiological importance and numerous etiological roles, GPCRs are the targets for more than 30% of all therapeutic drugs on the market.[4] A more nuanced mechanistic understanding of the GPCR activation landscape could dramatically expand their therapeutic value.[5]

Spectroscopic techniques such as fluorescence,[6] infrared,[7] electron paramagnetic resonance,[8] and nuclear magnetic resonance (NMR)[9] have revealed many lowly populated, high energy conformational states that remain invisible to X-ray crystallography and cryo-EM. In particular, the ability of NMR to access motional regimes covering more than 15 orders of magnitude (ps-s) makes it especially attractive for this task, although the challenges associated with uniform incorporation of NMR-active isotopes has somewhat limited its application.[10] Exogenous cysteine-reactive fluorine (^{19}F) probes have proven an effective alternative to uniform labeling[11–16] owing to their high gyromagnetic ratio (i.e., sensitivity), 100% natural abundance, large chemical shift range, and absence of background signals in biomolecular samples.[17] Yet, fluorine's intrinsically broad linewidths quickly lead to overlapping signals that require deconvolution, and generally prohibits the simultaneous labeling of multiple sites. Offsite ^{19}F-probe incorporation is an additional source of signal overlap that is specifically problematic when the target protein contains multiple cysteine residues that cannot be mutated because of their functional relevance.[9,18,19]

In our previous work, labeling the neurotensin receptor 1 (NTS1) Class A GPCR with cysteine-reactive 2-bromo-N-(4-[trifluoromethyl]phenyl)acetamide (^{19}F-BTFMA),[16] we uncovered a second source of offsite labeling: noncovalent sequestration by detergent proteomicelles. Conventional labeling methods solubilize the receptor in detergent micelles without the prior removal of excess ^{19}F-probe molecules. Our liquid-chromatography mass spectrometry (LC–MS) and NMR spectra of a cysteine-less NTS1 construct demonstrate that unreacted ^{19}F-BTFMA molecules are sequestered into proteomicelles. Subsequent detergent wash steps or detergent exchange is incapable of complete excess ^{19}F-BTFMA removal. We present a simple four-step protocol for Selective Labeling Absent of Probe Sequestration (SLAPS): physically disrupt cell membranes in the absence of detergent, incubate membranes with cysteine-reactive ^{19}F-BTFMA, remove excess unreacted ^{19}F-BTFMA molecules via ultracentrifugation, and finally solubilize in detergent of choice.

2 | RESULTS AND DISCUSSION

Several generations of thiol-reactive trifluoromethyl probes have been developed to study GPCR dynamics.[20–22] ^{19}F-BTFMA remains one of the most popular probes due to its ability to form a nonreducible thioether bond, along with high chemical shift sensitivity owing to aromatic ring polarizability (Figure 1a).[22] The majority of ^{19}F-GPCR studies conjugate probe to the intracellular tips of TM5,[23] TM6,[24] or TM7,[12] which have proven invaluable for mapping the receptor activation landscape due to their large architectural changes.[25] In many cases, this requires the introduction of a non-native cysteine residue at the position of interest and the simultaneous mutagenesis of all endogenous solvent-exposed cysteine residues that would lead to offsite labeling. Nonetheless, researchers have noted the presence of offsite ^{19}F-labeling in final protein samples.[9,18,19] These are commonly attributed to the numerous reduced cysteine residues in the TM region, although, this has rarely been experimentally verified (Figure 1b).

Spectroscopic studies require receptors to be isolated from the lipid membranes of the expression system and solubilized into detergent micelles for purification and, frequently, analysis. The ^{19}F-probes are typically incorporated following detergent solubilization of native lipid membranes, but prior to purification (herein referred to as the conventional ^{19}F-labeling protocol). We applied

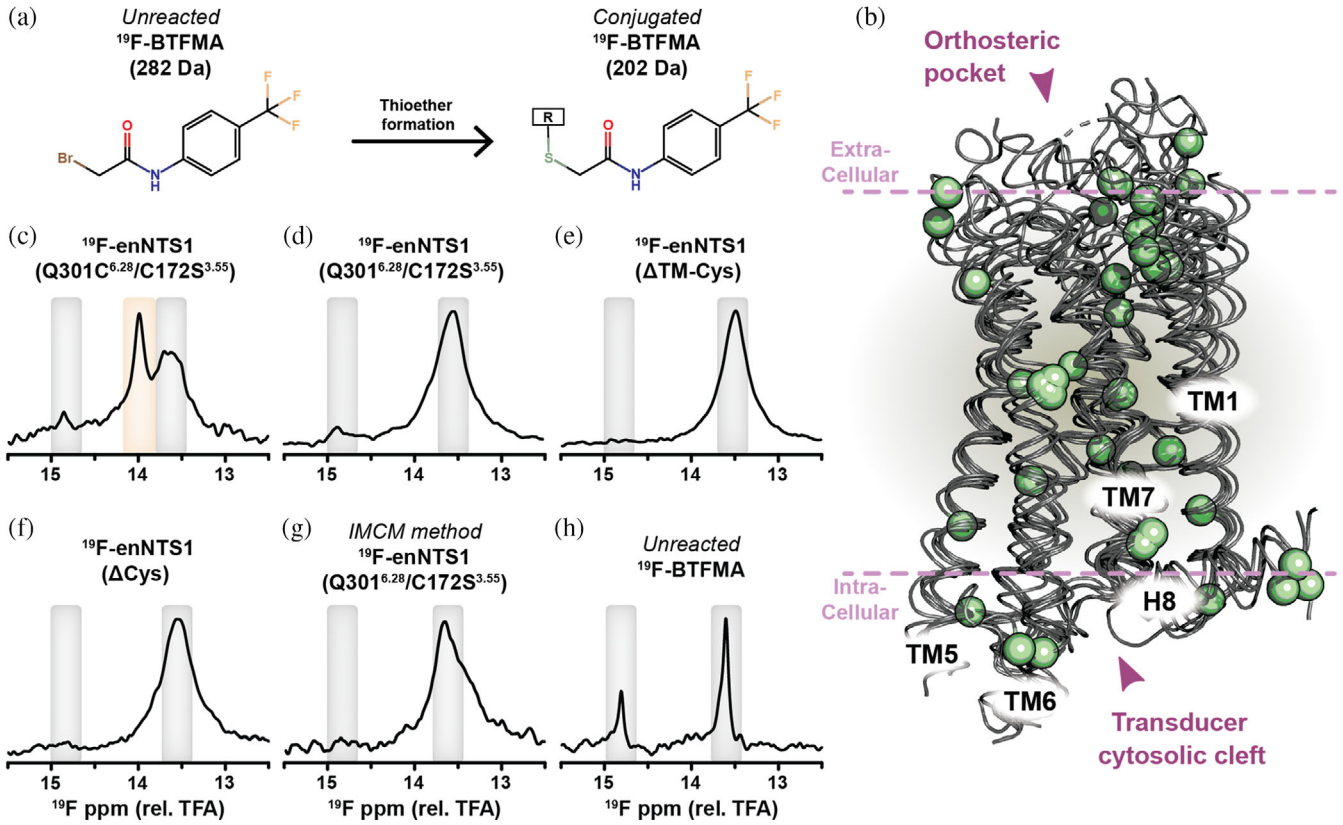

FIGURE 1 Labeling detergent-solubilized enNTS1 results in offsite ^{19}F-BTFMA probe incorporation. (a) Unreacted ^{19}F-BTFMA (*left*) conjugates to cysteine residues via thioether bond formation (*right*), adding +202 Da to receptor molecular weight. (b) Overlay of β_1-adrenergic (PDB 4BVN), β_2-adrenergic (PDB 2RH1), Adenosine A_{2A} (PDB 4EIY), Rhodopsin (PDB 1U19), and Neurotensin receptor 1 (PDB 4BWB) atomic models illustrates the numerous cysteine residues (green spheres) located throughout the extracellular, TM, and intracellular regions.[36–40] ^{19}F NMR spectra of (c) ^{19}F-enNTS1(Q301C$^{6.28}$/C172S$^{3.55}$), (d) ^{19}F-enNTS1(Q301$^{6.28}$/C172S$^{3.55}$), (e) ^{19}F-enNTS1(ΔTM-Cys), (f) ^{19}F-enNTS1(ΔCys), (g) ^{19}F-enNTS1(Q301$^{6.28}$/C172S$^{3.55}$) prepared by IMCM, and (h) unreacted ^{19}F-BTFMA. ^{19}F-chemical shifts are relative to TFA. All ^{19}F-enNTS1 samples were initially solubilized in DM detergent. Final sample buffer conditions for all NMR spectra: 20 mM HEPES, 50 mM NaCl, 50 μM TFA, and 0.01% (w/v) LMNG at pH 7.5. All NMR samples were supplemented with 10% (v/v) D_2O

this strategy to label a thermostabilized Neurotensin receptor 1 variant (enNTS1).[26] We introduced an exogenous cysteine on TM6 (Q301C$^{6.28}$, Ballesteros-Weinstein nomenclature[27]) and substituted the only solvent-exposed cysteine (C172S$^{3.55}$) to reduce offsite labeling, referring to the final construct as enNTS1(Q301C$^{6.28}$/C172S$^{3.55}$). Briefly, *Escherichia coli* cell pellets containing enNTS1 (Q301C$^{6.28}$/C172S$^{3.55}$) were resuspended in aqueous buffer, sonicated, solubilized with 1% (w/v) *n*-decyl-β-D-maltopyranoside (DM) detergent, and incubated for 1 h with ^{19}F-BTFMA. The sample was immobilized on metal-affinity resin for exchange to 2,2-didecylpropane-1,3-bis-β-D-maltopyranoside (LMNG) detergent micelles, then purified by cation exchange and gel filtration. The ^{19}F-enNTS1(Q301C$^{6.28}$/C172S$^{3.55}$) 1D ^{19}F NMR spectrum contained three resonances at 13.6, 14.0, and 14.8 ppm (Figure 1c). Many previous ^{19}F-GPCR studies reveal that TM6 exchanges between multiple conformations on the ms-s timescale; this would also produce a spectrum containing multiple peaks, even when the protein is ^{19}F-labeled at a single position (i.e., no offsite labeling).[9,13,16] As a negative control, we engineered ^{19}F-enNTS1 (Q301$^{6.28}$/C172S$^{3.55}$) with residue 301 reverted to glutamine and repeated the experiment. Surprisingly, the spectrum contained two resonances that were also present in the ^{19}F-enNTS1(Q301C$^{6.28}$/C172S$^{3.55}$) sample, which we interpreted as offsite cysteine reactions (Figure 1d).

We generated two additional cysteine-depleted enNTS1 constructs, enNTS1(ΔTM-Cys) and enNTS1 (ΔCys) to identify which cysteine residue was being labeled (Figure 2a); both constructs included C172S$^{3.55}$ and reverted residue 301$^{6.28}$ to glutamine. enNTS1 (Q301$^{6.28}$/C152S$^{3.35}$/C172S$^{3.55}$/C320S$^{6.47}$) eliminates the reduced cysteine residues from the TM region (C152S$^{3.35}$/C320S$^{6.47}$) while enNTS1(ΔCys) is entirely devoid of cysteines (C142S$^{3.25}$/C152S$^{3.35}$/C225S^{ECL2}/C320S$^{6.47}$). Both constructs were again ^{19}F-labeled following DM

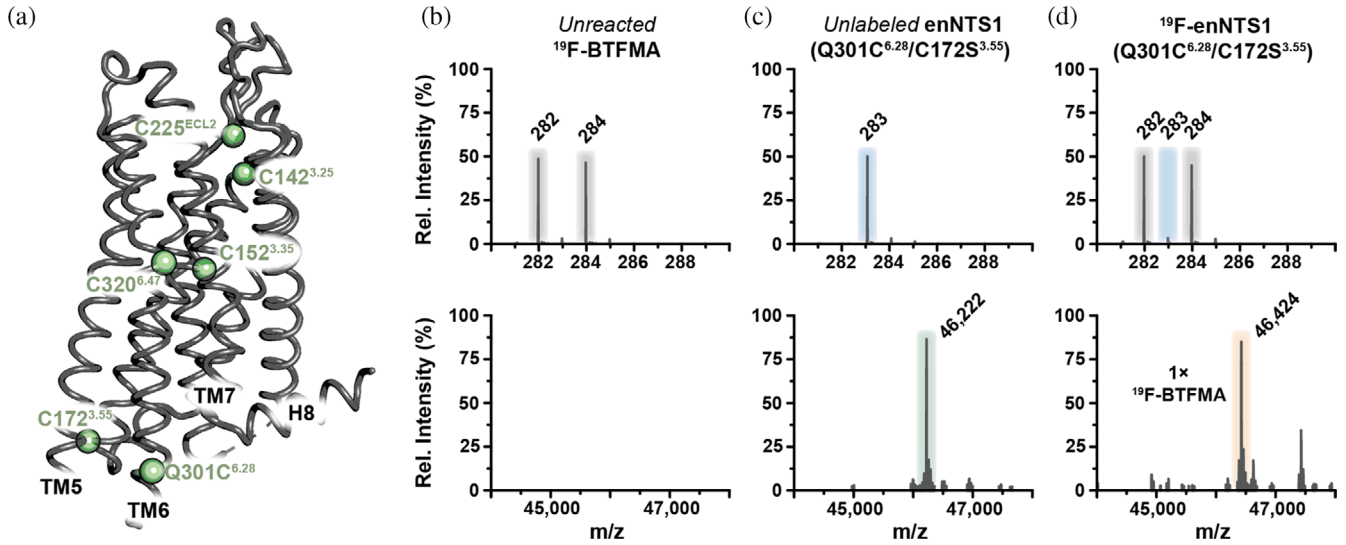

FIGURE 2 Detergent micelles sequester ^{19}F-BTFMA probe molecules. (a) Atomic model of enNTS1 (PDB 4BWB) highlighting cysteine residue mutations (green spheres).[36] LC–MS results of (b) ^{19}F-BTFMA, (c) unlabeled enNTS1(Q301C$^{6.28}$/C172S$^{3.55}$), and (d) ^{19}F-enNTS1 (Q301C$^{6.28}$/C172S$^{3.55}$). Both ^{19}F-enNTS1 samples (panels C and D) were initially solubilized in DM detergent. The final sample buffer conditions for all LC–MS spectra were 20 mM HEPES, 50 mM NaCl, 50 μM TFA, and 0.01% (w/v) LMNG at pH 7.5. All LC–MS peak intensities are relative to each individual spectrum. ^{19}F-BTFMA m/z = 282/284 Da; enNTS1(Q301C$^{6.28}$/C172S$^{3.55}$) m/z = 46,222 Da; ^{19}F-enNTS1(Q301C$^{6.28}$/C172S$^{3.55}$) m/z = 46,424 Da (1x ^{19}F-BTFMA molecule). A MW intensity of 283 Da was also observed in all enNTS1 protein samples, regardless of ^{19}F-BTFMA presence, corresponding to an unrelated sample contaminate

detergent solubilization and purified as above. Surprisingly, ^{19}F-enNTS1(ΔTM-Cys) and ^{19}F-enNTS1(ΔCys) spectra both contained a strong resonance at 13.6 ppm and a weaker one at 14.8 ppm as observed in the other ^{19}F-enNTS1 samples (Figure 1c–f). Wüthrich and colleagues recently showed that detergent-solubilized receptors were highly reactive and proposed the in-membrane chemical modification (IMCM) approach to reduce offsite labeling.[19] IMCM exploits the membrane's natural protection of TM cysteine residues by conjugating the probe following physical disruption of the lipid bilayer *but prior to* detergent solubilization. After probe incubation the receptor is solubilized in detergent and purified *without removal of excess probe*. We applied IMCM to our ^{19}F-enNTS1(Q301$^{6.28}$/C172S$^{3.55}$) negative control by incubating sonicated membranes with ^{19}F-BTFMA for 1 h prior to solubilization in DM micelles. However, we still observed a strong ^{19}F-resonance at 13.6 ppm (Figure 1g).

Next, we collected a spectrum of unreacted ^{19}F-BTFMA under the identical LMNG-containing NMR buffer conditions (Figure 1h). It contained the same two resonances at 13.6 and 14.8 ppm, but with substantially narrower linewidths than observed in the ^{19}F-enNTS1 samples consistent with a faster rotational correlation time for unreacted ^{19}F-BTFMA.[28] We assigned both ^{19}F resonances to ^{19}F-BTFMA. The commercially acquired ^{19}F-BTFMA also contains a triethylamine trihydrofluoride impurity as confirmed by 1D ^{1}H and ^{19}F NMR (Figure S1). Given that unreacted ^{19}F-BTFMA is considerably lipophilic with a theoretical octanol:water partition coefficient (logP) ~3.5,[29] we hypothesized that detergent proteomicelles may be sequestering excess ^{19}F-probe molecules. We turned to LC–MS to test this hypothesis. The reverse-phase LC step separates all non-covalent components of the proteomicelle for accurate determination of individual molecular weights. ^{19}F-BTFMA solubilized in detergent micelles showed the expected 282 and 284 Da Bromine isotope doublet pattern of the protonated, unreacted form (Figure 2b). Unlabeled enNTS1(Q301C$^{6.28}$/C172S$^{3.55}$) exhibited a prominent intensity of 46,222 Da (Figure 2c). LC–MS analysis of ^{19}F-enNTS1(Q301C$^{6.28}$/C172S$^{3.55}$) contained a major intensity of 46,424 Da, corresponding to conjugation of a single ^{19}F-BTFMA molecule (+202 Da), as well as the 282 and 284 Da doublet of unreacted ^{19}F-BTFMA (Figure 2d). Thus, the LC–MS illustrates that detergent proteomicelles can sequester unreacted ^{19}F-BTFMA.

To test if proteomicelle sequestration of unreacted ^{19}F-BTFMA molecules was a function of the DM detergent used during receptor solubilization, we solubilized two additional enNTS1(Q301$^{6.28}$/C172S$^{3.55}$) samples using either *n*-dodecyl-β-D-maltopyranoside (DDM) or LMNG detergent. Both of the enNTS1(Q301$^{6.28}$/C172S$^{3.55}$) samples were ^{19}F-labeled using the conventional method and then purified into the same final buffer containing LMNG as used earlier. Regardless of

the solubilization detergent identity, the 1D ^{19}F-spectra contained the same two peaks at 14.8 ppm and 13.6 ppm that were observed earlier for the DM solubilized receptors and the unreacted ^{19}F-BTFMA samples (Figure 1d–f, h and Figure S2(A,E)). Again, we employed intact and protease digestion LC–MS to confirm that enNTS1 (Q301$^{6.28}$/C172S$^{3.55}$) did not contain thioether-linked ^{19}F-BTFMA probes (Figure S2(B,F) and Tables S1 and S2). We prepared a trifluoroacetic acid (TFA) standard curve to quantitate the concentration of sequestered ^{19}F-BTFMA from ^{19}F resonance integrals. We measured concentrations of 13.8 and 35.2 μM for the peaks at 14.8 and 13.6 ppm, respectively. The sample contained 150 μM enNTS1(Q301$^{6.28}$/C172S$^{3.55}$) indicating ~0.33 ^{19}F-BTFMA molecules sequestered for every one receptor. Taken together, the conventional ^{19}F-labeling method results in proteomicelle sequestration of ^{19}F-BTFMA independent of the detergent used during receptor solubilization.

Next, we measured the longitudinal (T_1) and transverse (T_2) relaxation time parameters to test if they could serve as a straightforward criterion for the identification of sequestered ^{19}F-BTFMA probes. We collected T_1 inversion recovery and T_2 Carr-Purcell-Meiboom-Gill (CPMG) experiments on ^{19}F-enNTS1(Q301$^{6.28}$/C172S$^{3.55}$) initially solubilized in (i) DDM or (ii) LMNG detergent and then incubated with ^{19}F-BTFMA using the conventional method; the final detergent in these samples was LMNG. We determined a T_1 relaxation time parameter between 440 and 632 ms for the 14.8 ppm resonance and 508 and 570 ms for the 13.6 ppm resonance (Figure S2(C,G)); $T_{2;\text{homogenous}}$ relaxation time parameters ranged from 1.0 to 1.4 ms for the 14.8 resonance and 1.4 to 2.7 ms for the 13.6 ppm peak (Figure S2(D,H)). The measured relaxation times of proteomicelle sequestered ^{19}F-BTFMA are on the order of those measured for ^{19}F-BTFMA-conjugated receptors by us[16] and others.[9,13,30] In contrast, the linewidths at half height (LWHH) for the unreacted ^{19}F-BTFMA resonances at 14.8 and 13.6 ppm in empty LMNG detergent micelles are 37 and 47 Hz, respectively, making them easily discernable from both receptor-conjugated and proteomicelle sequestered ^{19}F-signals (Figures 1h and 3d). We estimate lower limits for the T_2 relaxation time parameter of 8.6 ms and 6.8 ms, respectively, using the equation $T_2 = 1/\pi\text{LWHH}$, with the assumption that there exists zero contribution from inhomogeneous T_2 relaxation or exchange broadening. Thus, we conclude that NMR cannot reliably discriminate proteomicelle sequestered ^{19}F-BTFMA from receptor-conjugated ^{19}F-BTFMA using chemical shift, T_1, or T_2 values. However, MS is able to

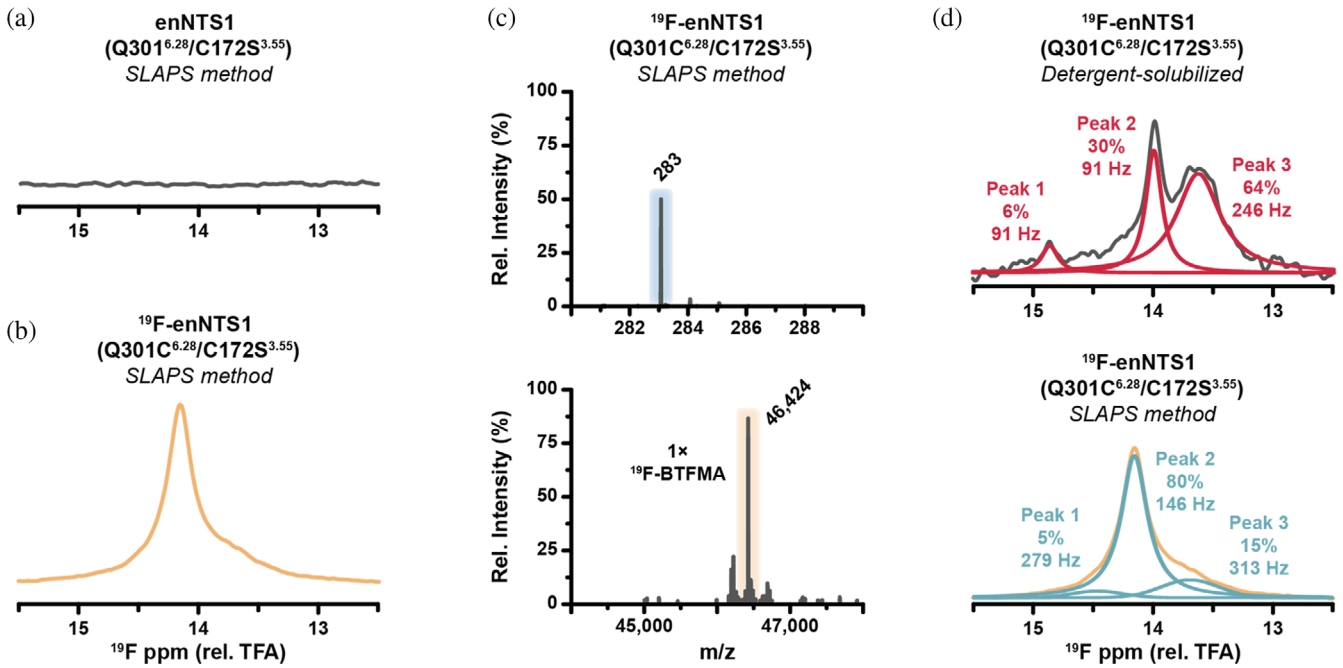

FIGURE 3 SLAPS eliminates offsite reactions in enNTS1. ^{19}F NMR spectra of (a) enNTS1(Q301$^{6.28}$/C172S$^{3.55}$) and (b) ^{19}F-enNTS1 (Q301C$^{6.28}$/C172S$^{3.55}$) prepared using the SLAPS protocol. Note that ^{19}F-BTFMA only reacts with enNTS1(Q301C$^{6.28}$/C172S$^{3.55}$). (c) LC–MS spectra of ^{19}F-enNTS1(Q301C$^{6.28}$/C172S$^{3.55}$) purified using SLAPS. Note the absence of unreacted ^{19}F-BTFMA (top). (d) MestReNova[35] spectral deconvolution of ^{19}F-enNTS1(Q301C$^{6.28}$/C172S$^{3.55}$) labeled while solubilized in DM detergent micelles (top) or using the SLAPS methodology (bottom). Final sample buffer conditions for all ^{19}F NMR spectra were 20 mM HEPES, 50 mM NaCl, 50 μM TFA, and 0.01% (w/v) LMNG at pH 7.5. All NMR samples were supplemented with 10% (v/v) D_2O

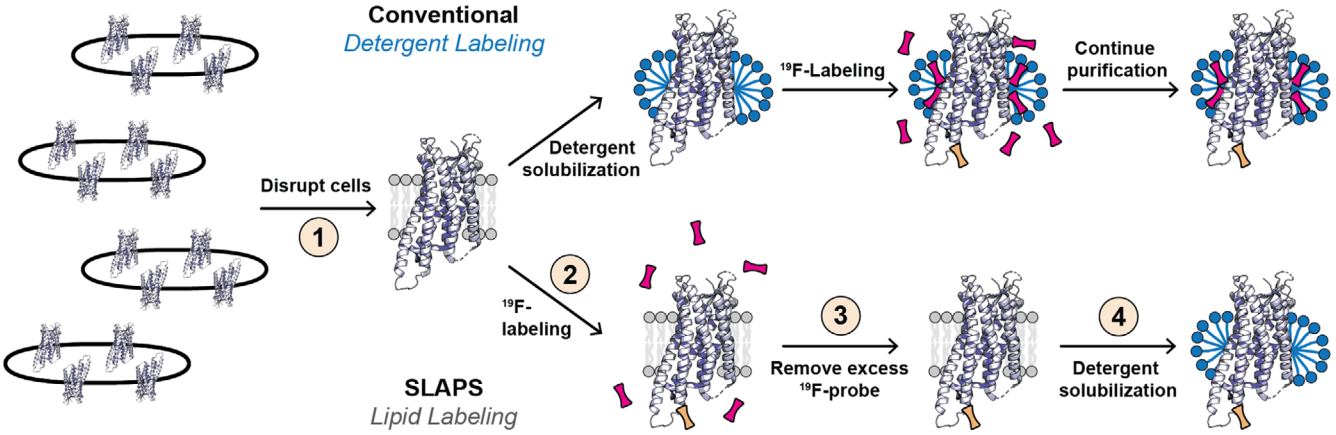

FIGURE 4 SLAPS protocol. (top) Model illustrating that receptors which are solubilized in detergent, prior to ^{19}F-labeling, will sequester unreacted probe molecules (red) in addition to the correctly conjugated probe (orange). SLAPS follows a simple four-step protocol: (1) physically disrupt cell membranes in the absence of detergent, (2) incubate membranes with cysteine-reactive ^{19}F-probes, (3) remove excess unreacted ^{19}F-probe molecules via ultracentrifugation, and (4) solubilize in the detergent of choice

reliably identify unreacted, proteomicelle sequestered ^{19}F-BTFMA in purified receptor samples.

We hypothesized that removal of excess, unreacted ^{19}F-BTFMA molecules via ultracentrifugation prior to detergent solubilization would eliminate proteomicelle sequestration. We sonicated cell pellets containing enNTS1(Q301$^{6.28}$/C172S$^{3.55}$), incubated for 1 h with ^{19}F-BTFMA, and then performed a membrane preparation via ultracentrifugation. The sample was pelleted at 100,000*g*, decanted, and washed with buffer containing no detergent. This ultracentrifugation step was repeated to ensure complete removal of excess ^{19}F-probe. The ^{19}F-enNTS1(Q301$^{6.28}$/C172S$^{3.55}$) sample was then solubilized with DM detergent and purified as above to produce a ^{19}F NMR spectrum with no observable signals (Figure 3a). Applying this methodology to ^{19}F-enNTS1 (Q301C$^{6.28}$/C172S$^{3.55}$) yielded a spectrum containing a single resonance in slow exchange (Figure 3b).[16] Intact and protease-digested LC–MS confirmed that ^{19}F-enNTS1 (Q301C$^{6.28}$/C172S$^{3.55}$) was exclusively labeled at Q301C$^{6.28}$ with no observable unreacted ^{19}F-BTFMA, and that ultracentrifugation prior to detergent solubilization is sufficient to remove unreacted ^{19}F-BTFMA (Figure 3c and Table S3). Spectral deconvolution of ^{19}F-enNTS1 (Q301C$^{6.28}$/C172S$^{3.55}$) prepared using the conventional method and SLAPS, without consideration of probe sequestration as a source of offsite labeling, would both be compatible with at least three receptor conformations in slow exchange (Figure 3d). Thus, we propose a simple four-step protocol for SLAPS: physically disrupt cell membranes in the absence of detergent, incubate membranes with cysteine-reactive ^{19}F-BTFMA, remove excess unreacted ^{19}F-BTFMA molecules via ultracentrifugation, and finally solubilize in detergent of choice (Figure 4).

3 | CONCLUSIONS

Conjugation of trifluoromethyl probes to GPCRs solubilized in detergent micelles is well known to result in offsite cysteine reactions. Here, we characterize a second source of offsite labeling: noncovalent probe sequestration by detergent micelles. Although our results suggest the IMCM approach is less effective at eliminating probe sequestration than it is at prohibiting offsite reactions,[19] there is one important consideration in our application of IMCM to enNTS1. The IMCM method was originally developed for the 2,2,2-triflouroethyl-1-thiol (^{19}F-TET) probe, which is considerably less lipophilic (logP ~1.5) than ^{19}F-BTFMA (logP ~3.5).[29] Therefore, we hypothesize that the IMCM approach would also limit detergent sequestration of ^{19}F-TET. Although, it may be less effective with the other more lipophilic probes such as 3-bromo-1,1,1-trifluoropropan-2-one (BTFA; logP ~2.0), 1-bromo-3,3,4,4,4-pentafluorobutan-2-one (BPFB; logP ~2.7), and N-(4-bromo-3-[trifluoromethyl]phenyl)acetamide (3-BTFMA; logP ~2.9).[22] It is also important to note that there are alternative approaches for selective ^{19}F-labeling that are inherently devoid of offsite labeling and detergent micelle sequestration. Aromatic amino acids (such as Tyr, Trp, or Phe) can be labeled simply by inclusion of their fluorinated-analogs in the expression medium.[31–33] Although, most GPCRs possess multiple aromatic residue that would ultimately lead to signal overlap within the 1D ^{19}F-spectrum. In a recently published manuscript, unnatural amino acid incorporation was used to ^{19}F-label the cannabinoid receptor 1 (CB1) in the baculovirus expression system, which may serve as a valuable tool for other eukaryotic membrane proteins.[15] Nonetheless, SLAPS is broadly applicable to a variety of

cysteine-reactive lipophilic probes, other GPCRs, and additional membrane protein classes solubilized in detergent micelles or lipid mimetics.

4 | MATERIALS AND METHODS

4.1 | enNTS1 plasmid construct and protein expression

The previously characterized functional variant $enNTS_1$[26] was available in an expression vector (termed pDS170) with an open reading frame encoding an N-terminal maltose-binding protein signal sequence (MBPss), followed by a 10x His tag, a MBP, a NNNNNNNNNNG linker and a HRV 3C protease site (LEVLFQGP), which were linked via a BamHI restriction site (resulting in additional residues GS) to residue T42 of the receptor. C-terminally T416 of the receptor was linked via a NheI restriction site (resulting in additional residues AS) to an Avi-tag for in vivo biotinylation, a HRV 3C protease site, a GGSGGS linker and a monomeric ultra-stable green fluorescent protein (muGFP).[34] enNTS1 plasmids were transformed into BL21(DE3) *E. coli* cells and plated overnight on LB agar supplemented with 100 μg/ml carbenicillin at 37°C. Liquid LB starter cultures were supplemented with 100 μg/ml carbenicillin, seeded with colonies, and incubated overnight at 37°C and 220 RPM. One-liter 2xYT media supplemented with 100 μg/ml carbenicillin and 0.3% (w/v) glucose were inoculated with overnight LB starter culture, and incubated at 37°C and 220 RPM to an $OD_{600} \cong 0.15$. The cultures were then cooled to 16°C. Once each culture reached an $OD_{600} \cong 0.6$, they were induced with 0.3 mM IPTG and incubated for ~21 h at 16°C and 220 RPM. The cultures were harvested via centrifugation at 4,000*g* and stored at −80°C.

4.2 | Conventional ^{19}F-labeling protocol

Cell pellets were solubilized on ice in *solubilization buffer* (100 mM HEPES, 400 mM NaCl, 20% [v/v] glycerol, 10 mM $MgCl_2$, 10 mM imidazole, pH 8.0), 100 mg lysozyme, 1-unit DNAse, 0.2 mM PMSF, and one protease inhibitor cocktail tablet. Solution was then sonicated on ice 2 min processing time (10 s on, 20 s off) at 30% maximum amplitude. Following sonication, the receptor sample was solubilized at a final concentration of 0.6% (w/v) CHAPS, 0.12% (w/v) CHS, 1% (w/v) DM detergent, 5 mM ^{19}F-BTFMA (~20,000:1 ^{19}F-BTFMA:enNTS1), and 0.2 mM PMSF. The solution was stirred at 4°C for 2 h. After incubation, 16 mg aldrithiol was added to the solution and stirred at 4°C for an additional 10 min. Insoluble material was removed by centrifugation at 24,424*g* for 45 min, then subsequently purified as described in the "*enNTS1 protein purification*" Methods section.

4.3 | IMCM ^{19}F-labeling protocol

Cell pellets were solubilized on ice in *solubilization buffer* (100 mM HEPES, 400 mM NaCl, 20% [v/v] glycerol, 10 mM $MgCl_2$, 10 mM imidazole, pH 8.0), 100 mg lysozyme, 1-unit DNAse, 0.2 mM PMSF, and one protease inhibitor cocktail tablet. Solution was then sonicated on ice 2 min processing time (10 s on, 20 s off) at 30% maximum amplitude. Following sonication, 5 mM ^{19}F-BTFMA (~20,000:1 ^{19}F-BTFMA:enNTS1) and 0.2 mM PMSF was added to the solution and stirred at 4°C for 1 h. After incubation, 16 mg aldrithiol was added to the solution and stirred at 4°C for an additional 10 min. Next, the receptor sample was solubilized at a final concentration of 0.6% (w/v) CHAPS, 0.12% (w/v) CHS, and 1% (w/v) DM detergent. The solution was stirred at 4°C for 2 h. Insoluble material was removed by centrifugation at 24,424*g* for 45 min, then subsequently purified as described in the "*enNTS1 protein purification*" Methods section.

4.4 | SLAPS ^{19}F-labeling protocol

Cell pellets were solubilized on ice in *solubilization buffer* (100 mM HEPES, 400 mM NaCl, 20% [v/v] glycerol, 10 mM $MgCl_2$, 10 mM imidazole, pH 8.0), 100 mg lysozyme, 1-unit DNAse, 0.2 mM PMSF, and one protease inhibitor cocktail tablet. Solution was then sonicated on ice: 2 min processing time (10 s on, 20 s off) at 30% maximum amplitude. Following sonication, 5 mM ^{19}F-BTFMA (~20,000:1 ^{19}F-BTFMA:enNTS1) and 0.2 mM PMSF was added to the solution and stirred at 4°C for 1 h. After incubation, 16 mg aldrithiol was added to the solution and stirred at 4°C for an additional 10 min. The following ultracentrifugation steps are unique to the SLAPS method: To remove excess ^{19}F-BTFMA probe, a membrane preparation was performed via ultracentrifugation at 100,000*g* for 10 min. The supernatant was decanted and the pellet was resuspended in the same volume of fresh *solubilization buffer*. A second membrane preparation was performed via ultracentrifugation at 100,000*g* for 10 min. Following ultracentrifugation, the receptor sample was solubilized at a final concentration of 0.6% (w/v) CHAPS, 0.12% (w/v) CHS, and 1% (w/v) DM detergent. The solution was stirred at 4°C for

2 h. Insoluble material was removed by centrifugation at 24,424*g* for 45 min, then subsequently purified as described in the "*enNTS1 protein purification*" Methods section.

4.5 | enNTS1 protein purification

The remaining enNTS1 supernatant was then incubated with *equilibrated TALON* resin (25 mM HEPES, 10% (v/v) glycerol, 300 mM NaCl, 0.15% (w/v) DM, pH 8.00) at 4°C for 15 min. Following TALON resin binding, the receptor solution was placed into a gravity column to remove unbound proteins. The TALON resin was then subjected to two subsequent wash steps: *TALON wash #1* (25 mM HEPES, 10% (v/v) glycerol, 500 mM NaCl, 0.15% (w/v) DM, 10 mM Imidazole, 4 mM ATP, 10 mM MgCl2, pH 8.0) and *TALON wash #2* (25 mM HEPES, 10% (v/v) glycerol, 350 mM NaCl, 0.1% (w/v) LMNG, 10 mM Imidazole, pH 8.0). It is important to note that the second wash step also serves as a detergent exchange step from DM to LMNG. Following detergent exchange, enNTS1 was eluted with *TALON elute buffer* (25 mM HEPES, 10% (v/v) glycerol, 500 mM NaCl, 0.01% (w/v) LMNG, 350 mM Imidazole, pH 8.0) and incubated with 3 mg 3C precision protease for 2–16 h at 4°C to remove MBP and muGFP expression tags. The cleaved enNTS1 was concentrated in a 50 MWCO concentrator via centrifugation at 3,500*g* and then diluted 10-fold in *SP equilibration buffer* (20 mM HEPES, 10% (v/v) glycerol, 0.01% (w/v) LMNG, pH 7.4). This resulting solution was loaded onto an equilibrated 5 ml SP ion-exchange (IEX) column via GE AKTA Pure system. The SP IEX column was washed with *SP wash buffer* (20 mM HEPES, 10% (v/v) glycerol, 250 mM NaCl, 0.01% (w/v) LMNG, pH 7.4) until the AU_{280} stabilized. An equilibrated 1 ml Ni^{2+}-NTA column was attached in-tandem following the 5 ml SP IEX column, and the receptor eluted with *SP elute buffer* (20 mM HEPES, 10% (v/v) glycerol, 1 M NaCl, 0.01% (w/v) LMNG, 25 mM Imidazole, pH 7.4). The enNTS1 solution was then concentrated in a 50 MWCO concentrator via centrifugation at 3,500*g* and injected onto a GE S200 Increase SEC column equilibrated in *NMR buffer* (20 mM HEPES, 50 mM NaCl, 0.01% (w/v) LMNG, 50 μM TFA, pH 7.5). Following SEC, the desired enNTS1 fractions were pooled, concentrated to 100–300 μM, and flash-frozen via liquid nitrogen and stored at −80°C.

4.6 | ^{19}F NMR

^{19}F NMR spectra were collected on a 14.1 T Bruker AVANCE NEO (Indiana University, Bloomington) or Bruker AVANCE HD 14.1 T (Indiana University School of Medicine) spectrometer equipped with a 5 mm TCI CryoProbe tunable to the fluorine frequency. Free induction decay (FID) signals were collected by applying a π/2 pulse length of 13.5 μs, a recycling time of 0.8 s, and an acquisition time of 0.15 s. A total of 8,192 scans were collected generating a FID comprised of 2,499 complex points, which were zero-filled to 8,000 complex points, and apodized with a 30 Hz exponential function. T_1 inversion recovery and T_2 CPMG experiments were collected in a fully interleaved fashion to account for protein degradation effects on peak intensities/height. T_1 experiments were collected with variable delays between 50 and 1,000 ms and a recovery delay of 2 s. The normalized peak heights of the deconvoluted inversion recovery T_1 spectra were fit to a monoexponential model. T_2 experiments were collected using a train of 1 ms CPMG spin-echo periods over a 1–6 ms total delay and the normalized peak heights of the deconvoluted CPMG T_2 spectra were fit to a monoexponential model. NMR spectra were deconvoluted using MestReNova as previously detailed.[16,35]

4.7 | ^{1}H NMR

^{1}H NMR spectra were collected on a 14.1 T Bruker AVANCE NEO (Indiana University, Bloomington) spectrometer equipped with a 5 mm TCI CryoProbe. FID signals were collected by applying a π/2 pulse length of 7.15 μs, a recycling time of 1 s, and an acquisition time of 0.72 s. A total of 64 scans were collected generating a FID comprised of 16 k complex points, which were zero-filled to 128 k complex points, and processed with a cosine-squared window function using MestReNova.[16,35]

4.8 | Mass spectrometry

4.8.1 | Intact protein analysis

Samples were analyzed on a Synapt G2S equipped with an iClass Acquity HPLC (Waters). Buffer A was 0.1% (v/v) formic acid in water and Buffer B was 0.1% (v/v) formic acid in acetonitrile. Proteins were separated using a 9-min gradient from 5% to 99% Buffer B at a flow rate of 50 nl/min. Proteins were separated using a 5 cm × 0.5 mm column in-house packed with Jupiter 5 μm C4 resin (Phenomenex). The time-of-flight (ToF) was set to positive ion mode and the analyzer mode was set to "resolution." The mass range was set to 100–1,500 Da with a scan time of 1 s and data collected in continuum mode. The electrospray capillary voltage was

set to 3.0 kV. The source and desolvation temperatures were 120°C and 350°C, respectively. The resulting LC–MS data was summed across the protein elution window. The resulting spectra were smoothed with a Savitzky–Golay filter with a window of four and two iterations. The protein charge state envelope was deconvoluted using MaxEnt1 in the Waters software.

4.8.2 | Protein digestion for peptimass spectrometry

Samples were resuspended and denatured in 8 M urea with 100 mM ammonium bicarbonate (pH 7.8). Disulfide bonds were reduced by incubation for 45 min at 57°C with a final concentration of 10 mM Tris (2-carboxyethyl) phosphine hydrochloride (#C4706, Sigma Aldrich). A final concentration of 20 mM iodoacetamide (#I6125, Sigma Aldrich) was then added to alkylate these side chains and the reaction was allowed to proceed for 1 h in the dark at 21°C. Samples were diluted to 1 M urea using 100 mM ammonium bicarbonate, pH 7.8. Trypsin (V5113, Promega) or chymotrypsin (#11418467001, Sigma Aldrich) was added at a 1:100 ratio and the samples were digested for 14 h at 37°C.

4.8.3 | Peptide ass spectrometry

Individual samples were desalted using ZipTip pipette tips (EMD Millipore), dried down and resuspended in 0.1% (v/v) formic acid. Fractions were analyzed by LC–MS on an Orbitrap Fusion Lumos equipped with an Easy NanoLC1200 HPLC (Thermo Fisher Scientific). Buffer A was 0.1% (v/v) formic acid in water. Buffer B was 0.1% (v/v) formic acid in 80% acetonitrile. Peptides were separated on a 30-min gradient from 0% to 3% Buffer B. Precursor ions were measured in the Orbitrap with a resolution of 120,000. Fragment ions were measured in the Orbitrap with a resolution of 15,000. The spray voltage was set at 1.8 kV. Orbitrap MS1 spectra (AGC 1×10^6) were acquired from 350 to 2,000 m/z followed by data-dependent HCD MS/MS (collision energy 30%, isolation window of 2 Da) for a 3 s cycle time. Charge state screening was enabled to reject unassigned and singly charged ions. A dynamic exclusion time of 30 s was used to discriminate against previously selected ions.

4.8.4 | Database search

The LC–MS/MS data was searched against the protein sequence using Protein Prospector (v5.22.1). The database search parameters for the tryptic search allowed for two missed cleavages and one nontryptic cleavage. The search parameters for the chymotryptic search allowed for four missed cleavages and one nonchymotryptic cleavage. A precursor and fragment mass tolerance of 10 ppm was used. Oxidation of methionine, pyroglutamine on peptide amino termini, carbamidomethylation of cysteine, and protein N-terminal acetylation were set as variable modifications. In addition, modification of cysteine residues by conjugated ^{19}F-BTFMA ($C_9H_6F_3NO$) was set as a variable modification.

AUTHOR CONTRIBUTIONS

Austin D. Dixon: Data curation (equal); formal analysis (equal); investigation (equal); writing – original draft (lead); writing – review and editing (equal). **Scott A. Robson:** Formal analysis (supporting); methodology (supporting); writing – original draft (supporting); writing – review and editing (supporting). **Jonathan C. Trinidad:** Data curation (equal); formal analysis (equal); methodology (supporting); writing – original draft (supporting).

ACKNOWLEDGMENTS

We are grateful to Dr. Hongwei Wu at Indiana University for NMR instrument assistance, Dr. Ratan Rai at Indiana University School of Medicine for NMR instrument assistance, and Prof. Daniel Scott at the Florey Institute for providing the enNTS1 plasmid used in this study. We appreciate the constructive feedback from James Bower, Thomas Shriver, and Skylar Zemmer. The project was funded by Indiana Precision Health Initiative (JJZ) and NIH (Grant/Award Numbers: R00GM115814 (JJZ) and R35GM143054 (JJZ)). The 14.1 T spectrometers used in this study were generously supported by the Indiana University Fund.

DATA AVAILABILITY STATEMENT

Data will be available upon reasonable request.

ORCID

Austin D. Dixon https://orcid.org/0000-0001-8676-915X
Scott A. Robson https://orcid.org/0000-0002-0529-0399
Jonathan C. Trinidad https://orcid.org/0000-0002-8279-1509
Joshua J. Ziarek https://orcid.org/0000-0002-3740-9999

REFERENCES

1. de Mendoza A, Sebé-Pedrós A, Ruiz-Trillo I. The evolution of the GPCR signaling system in eukaryotes: Modularity, conservation, and the transition to metazoan multicellularity. Genome Biol Evol. 2014;6:606–619.
2. Hanlon CD, Andrew DJ. Outside-in signaling – A brief review of GPCR signaling with a focus on the drosophila GPCR family. J Cell Sci. 2015;128:3533–3542.

3. Schönegge A-M, Gallion J, Picard L-P, et al. Evolutionary action and structural basis of the allosteric switch controlling β2AR functional selectivity. Nat Commun. 2017;8:2169.
4. Hauser AS, Attwood MM, Rask-Andersen M, Schiöth HB, Gloriam DE. Trends in GPCR drug discovery: New agents, targets and indications. Nat Rev Drug Discov. 2017;16:829–842.
5. Lu S, He X, Yang Z, et al. Activation pathway of a G protein-coupled receptor uncovers conformational intermediates as targets for allosteric drug design. Nat Commun. 2021;12:4721.
6. Zhou Y, Meng J, Xu C, Liu J. Multiple GPCR functional assays based on resonance energy transfer sensors. Front Cell Dev Biol. 2021;9:611443.
7. Ye S, Zaitseva E, Caltabiano G, et al. Tracking G-protein-coupled receptor activation using genetically encoded infrared probes. Nature. 2010;464:1386–1389.
8. Manglik A, Kim TH, Masureel M, et al. Structural insights into the dynamic process of β2-adrenergic receptor signaling. Cell. 2015;161:1101–1111.
9. Kim TH, Chung KY, Manglik A, et al. The role of ligands on the equilibria between functional states of a G protein-coupled receptor. J Am Chem Soc. 2013;135:9465–9474.
10. Verardi R, Traaseth NJ, Masterson LR, Vostrikov VV, Veglia G. Isotope labeling for solution and solid-state NMR spectroscopy of membrane proteins. Adv Exp Med Biol. 2012;992:35–62.
11. Frei JN, Broadhurst RW, Bostock MJ, et al. Conformational plasticity of ligand-bound and ternary GPCR complexes studied by 19F NMR of the β1-adrenergic receptor. Nat Commun. 2020;11:669.
12. Liu JJ, Horst R, Katritch V, Stevens RC, Wüthrich K. Biased signaling pathways in β2-adrenergic receptor characterized by 19F-NMR. Science. 2012;335:1106–1110.
13. Sušac L, Eddy MT, Didenko T, Stevens RC, Wüthrich K. A2A adenosine receptor functional states characterized by 19F-NMR. Proc Natl Acad Sci. 2018;115:12733–12738.
14. Klein-Seetharaman J, Getmanova EV, Loewen MC, Reeves PJ, Khorana HG. NMR spectroscopy in studies of light-induced structural changes in mammalian rhodopsin: Applicability of solution 19F NMR. Proc Natl Acad Sci. 1999;96:13744–13749.
15. Wang X, Liu D, Shen L, et al. A genetically encoded F-19 NMR probe reveals the allosteric modulation mechanism of cannabinoid receptor 1. J Am Chem Soc. 2021;143:16320–16325.
16. Dixon AD, Inoue A, Robson SA, et al. Effect of ligands and transducers on the Neurotensin receptor 1 conformational ensemble. J Am Chem Soc. 2022;144:10241–10250.
17. Chen H, Viel S, Ziarelli F, Peng L. 19F NMR: A valuable tool for studying biological events. Chem Soc Rev. 2013;42:7971–7982.
18. Staus DP, Wingler LM, Pichugin D, Prosser RS, Lefkowitz RJ. Detergent- and phospholipid-based reconstitution systems have differential effects on constitutive activity of G-protein-coupled receptors. J Biol Chem. 2019;294:13218–13223.
19. Sušac L, O'Connor C, Stevens RC, Wüthrich K. In-membrane chemical modification (IMCM) for site-specific chromophore labeling of GPCRs. Angew Chem Int Ed Engl. 2015;54:15246–15249.
20. Klein-Seetharaman J, Oikawa M, Grimshaw SB, et al. Long-range interactions within a nonnative protein. Science. 2002;295:1719–1722.
21. Luchette PA, Prosser RS, Sanders CR. Oxygen as a paramagnetic probe of membrane protein structure by cysteine mutagenesis and (19)F NMR spectroscopy. J Am Chem Soc. 2002;124:1778–1781.
22. Ye L, Larda ST, Frank Li YF, Manglik A, Prosser RS. A comparison of chemical shift sensitivity of trifluoromethyl tags: Optimizing resolution in ^{19}F NMR studies of proteins. J Biomol NMR. 2015;62:97–103.
23. Mulry E, Ray AP, Eddy MT. Production of a human histamine receptor for NMR spectroscopy in aqueous solutions. Biomolecules. 2021;11:11.
24. Eddy MT, Didenko T, Stevens RC, Wüthrich K. β2-adrenergic receptor conformational response to fusion protein in the third intracellular loop. Structure. 2016;24:2190–2197.
25. Sanchez-Soto M, Verma RK, Willette BKA, et al. A structural basis for how ligand binding site changes can allosterically regulate GPCR signaling and engender functional selectivity. Sci Signal. 2020;13(617):eaaw5885.
26. Bumbak F, Keen AC, Gunn NJ, Gooley PR, Bathgate RAD, Scott DJ. Optimization and 13CH3 methionine labeling of a signaling competent neurotensin receptor 1 variant for NMR studies. Biochim Biophys Acta Biomembr. 2018;1860:1372–1383.
27. Ballesteros JA, Weinstein H. Integrated methods for the construction of three-dimensional models and computational probing of structure-function relations in G protein-coupled receptors. Recept Mol Biol. 1995;25:366–428.
28. Cavanagh J, Fairbrother WJ, Palmer AG, Rance M, Skelton NJ. Classical NMR spectroscopy. Burlington: Academic Press, 2007;p. 1–28.
29. ChemAxon. MarvinSketch was used for calculating logP partition coefficients, MarvinSketch version 20.17.0. Budapest, Hungary: ChemAxon, 2020.
30. Ye L, Van Eps N, Zimmer M, Ernst OP, Scott Prosser R. Activation of the A2A adenosine G-protein-coupled receptor by conformational selection. Nature. 2016;533:265–268.
31. Gerig JT. Fluorine NMR of proteins. Prog Nucl Magn Reson Spectrosc. 1994;26:293–370.
32. Mishra NK, Urick AK, Ember SWJ, Schönbrunn E, Pomerantz WC. Fluorinated aromatic amino acids are sensitive 19F NMR probes for Bromodomain-ligand interactions. ACS Chem Biol. 2014;9:2755–2760.
33. Li H, Frieden C. NMR studies of 4-19F-phenylalanine-labeled intestinal fatty acid binding protein: Evidence for conformational heterogeneity in the native state. Biochemistry. 2005;44:2369–2377.
34. Scott DJ, Gunn NJ, Yong KJ, et al. A novel ultra-stable, monomeric green fluorescent protein for direct volumetric imaging of whole organs using CLARITY. Sci Rep. 2018;8:667.
35. Willcott MR. MestReNova. J Am Chem Soc. 2009;131:13180.
36. Miller-Gallacher JL, Nehmé R, Warne T, et al. The 2.1 Å resolution structure of Cyanopindolol-bound β1-Adrenoceptor identifies an intramembrane Na+ ion that Stabilises the ligand-Free receptor. PLoS One. 2014;9:e92727.
37. Vadim C, Rosenbaum DM, Hanson MA, et al. High-resolution crystal structure of an engineered human β2-adrenergic G protein–coupled receptor. Science. 2007;318:1258–1265.
38. Wei L, Chun E, Thompson AA, et al. Structural basis for allosteric regulation of GPCRs by sodium ions. Science. 2012;337:232–236.
39. Okada T, Sugihara M, Bondar A-N, Elstner M, Entel P, Buss V. The retinal conformation and its environment in rhodopsin in light of a new 2.2Å crystal structure. J Mol Biol. 2004;342:571–583.
40. Egloff P, Hillenbrand M, Klenk C, et al. Structure of signaling-competent neurotensin receptor 1 obtained by directed

evolution in Escherichia coli. Proc Natl Acad Sci. 2014;111: E655–E662.

SUPPORTING INFORMATION

Additional supporting information can be found online in the Supporting Information section at the end of this article.

How to cite this article: Dixon AD, Robson SA, Trinidad JC, Ziarek JJ. A method for selective ^{19}F-labeling absent of probe sequestration (SLAPS). Protein Science. 2022;31(11):e4454. https://doi.org/10.1002/pro.4454